Excited-State Dynamics of *pharaonis* Phoborhodopsin Probed by Femtosecond Fluorescence Spectroscopy†

Hideki Kandori*

Department of Applied Chemistry, Nagoya Institute of Technology, Showa-ku, Nagoya 466-8555, Japan

Hiroaki Tomioka

Department of Chemistry, Faculty of Education, Saitama University, 255 Shimo-Ohokubo, Saitama 338-8570, Japan

Hiroyuki Sasabe

Department of Photonics Materials Science, Chitose Institute of Science & Technology, 758-65 Bibi, Chitose, Hokkaido 066-8655, Japan

Received: June 26, 2001; In Final Form: November 6, 2001

Femtosecond time-resolved fluorescence spectroscopy has been used to study the excited-state dynamics of *pharaonis* phoborhodopsin (*p*pR) from *Natronobacterium pharaonis*. Upon excitation of *p*pR with a femtosecond pulse (444 nm), fluorescence decay kinetics are measured in the wavelengths between 488 and 678 nm. The obtained kinetics are strongly dependent on the probing wavelengths, and the decay components are approximately classified into the femtosecond (80−250 fs) and early picosecond (1.7−3.0 ps) components. The lifetimes are similar to those for the chromophore (a protonated Schiff base of all-trans retinal; AT-PSB) in methanol solution (90−800 fs and 2.5−3.7 ps) [Kandori, H.; Sasabe, H. *Chem. Phys. Lett.* **1993**, *216*, 126−132], implying that rapid deactivation from the excited state in rhodopsins is essentially part of the nature of the chromophore itself. In contrast, the femtosecond component is more predominant in the protein environment of *p*pR than in solution. Together with their quantum yields of photoisomerization (0.5 for *p*pR and 0.15 for AT-PSB in methanol) and product formation time in the recent pump−probe measurement of *p*pR [Lutz et al. *Proc. Natl. Acad. Sci. U.S.A.* **2001**, *98*, 962−967], we concluded that the femtosecond components correspond to highly efficient photoisomerization through barrierless transition in the excited-state whose quantum yield is close to unity. On the other hand, picosecond components are correlated with deactivation processes back to the ground state of *p*pR, whose isomerization quantum yield is low. Highly organized protein matrix could concentrate the excited molecules into the reaction coordinate for photoisomerization.

Rhodopsins possess a retinal molecule as the chromophore and a photon absorption triggers cis−trans isomerization of the retinal chromophore, which then leads to protein structural changes for light-signal and light-energy conversions.[1−5] By use of ultrafast spectroscopies, we now know that the primary cis−trans isomerization takes place very rapidly from the initially excited state.[3,5] Such rapid reaction can overcome the other relaxation processes back to the original state, and highly efficient photoconversion system is realized in proteins. Efficient photoisomerization in proteins can be described by their quantum yields of photoisomerization. The quantum yields in rhodopsins (0.67 for visual rhodopsin;[6] 0.6−0.65 for bacteriorhodopsin;[7,8] 0.5 for *pharaonis* phoborhodopsin[9]) are greater than those of the chromophore (a protonated Schiff base of retinal; PSB) in solution (∼0.15[10−12]). This fact suggests that photoisomerization of the retinal chromophore in proteins takes place more quickly than in solution.

PSB in solution can be considered as a good reference system of rhodopsins for studying interactions with surrounding molecules. In proteins, the PSB molecule interacts specifically with surrounding amino acid residues fixed into the protein coordinate. On the other hand, in solution, surrounding solvent molecules possess a greater degree of freedom than amino acid residues of proteins. Therefore, excited-state dynamics could be different between rhodopsins and PSB in solution, and a faster isomerization channel may be open for rhodopsins. In the previous reports, however, we showed that fluorescence lifetimes of PSB in solution are also short.[13,14] The lifetimes of the protonated Schiff base of all-trans retinal (AT-PSB) in methanol distribute between 90 fs and 3.7 ps, where kinetics could be fitted by femtosecond and early picosecond components.[13] Similarly, the lifetimes of the protonated Schiff base of 11-cis retinal (PSB11) contained both femtosecond (90−600 fs) and early picosecond (2−3 ps) components.[14] Thus, a detailed comparative investigation of PSB between the protein matrix and solution phase is important to understand the molecular mechanism of specific photoisomerization processes in rhodopsins.

In this paper, we show the femtosecond fluorescence spectroscopy of *pharaonis* phoborhodopsin from *Natronobacterium pharaonis* (*p*pR; also called *p*sRII), whose measurements are

† Part of the special issue "Norboru Mataga Festschrift".

* To whom correspondence should be addressed. E-mail: kandori@ach.nitech.ac.jp.

10.1021/jp012447f CCC: $22.00
Published on Web 02/16/2002

carried out under the identical experimental setup for AT-PSB in solution.[13] The *p*pR molecule has very similar absorption properties to those of phoborhodopsin (pR) of *Halobacterium salinarum*, the fourth retinal protein other than bacteriorhodopsin (bR), halorhodopsin (hR), and sensory rhodopsin (sR). Both *p*pR and pR are responsible for the negative phototaxis of each archaebacterium.[15,16] Like the other archaeal rhodopsins, *p*pR has all-trans retinal as its chromophore,[17] whereas *p*pR and pR possess orange-color (λ_{max}: ~500 nm) unlike the other purple-colored archaeal rhodopsins (bR, hR and sR; λ_{max}: 570~580 nm).[18]

Recently femtosecond pump−probe spectroscopy was applied to *p*pR at ~30 fs resolution.[19] The spectral and temporal absorption changes between 400 and 890 nm were interpreted in terms of the following sequential scheme; <150 fs for the transition from the excited Franck−Condon state to the relaxed state, 300 fs for the transition from the excited state to the J intermediate, and 4−5 ps for the transition from the J intermediate to the K intermediate. Nevertheless, the present fluorescence spectroscopy clearly showed the presence of the 2−3 ps component in addition to the <300 fs component as the lifetimes of the excited state of *p*pR. Kinetic comparison with AT-PSB in solution further revealed that the excited-state dynamics in *p*pR is essentially part of the nature of the chromophore itself, whereas the femtosecond processes are more populated in protein.

Experimental Section

A. Sample Preparation. The type strain of *Natronobacterium pharaonis*, DSM2160, was obtained from the culture collection DSM (Deutsche Sammlung von Mikroorganismen). The harvested cells were disrupted by freeze and thaw. Membrane fraction was collected by centrifugation at 140 000 × g for 60 min at 4 °C. The membrane fraction was washed with 4 M NaCl until the supernatant became clear, followed by solubilization with sodium cholate buffer. Chromatographic separation procedures was previously described in detail.[20] *p*pR was purified with four column chromatographic separations. Elution of *p*pR from first column was performed with octylglucoside buffer.

The purified *p*pR sample was dialyzed against for pure water. After 48 h dialysis, the precipitated *p*pR sample was collected by centrifugation at 15 000 × g for 10 min at 4 °C. The *p*pR sample was dissolved with 0.5% octylglucoside-4 M NaCl-25 mM PIPES (pH7.2). An undissolved pellet was removed by centrifugation at 15 000 × g for 5 min at 4 °C. The clear supernatant was used for spectroscopic measurement.

B. Femtosecond Up-Conversion Apparatus. A femtosecond up-conversion apparatus was used to measure the fluorescence decay of *p*pR as described.[13,14,21,22] The light source was an Ar^+ laser pumped mode-locked Ti:Sapphire laser with control of group velocity dispersion (GVD) by a prism pair (Tsunami, Spectra-Physics). The output power, central wavelength, and repetition rate were 800 mW, 888 nm, and 82 MHz, respectively. The pulse width was determined to be about 100 fs by an autocorrelation measurement.

The second harmonic (444 nm) was generated by focusing the linearly polarized laser output into a phase-matched 0.3 mm BBO crystal and used to excite the *p*pR sample. The *p*pR sample of 200 μL volume was put in a 1 mm path cell, and the electric brush was used to stir the sample during the experiments. The excitation power was 70 mW, corresponding to 0.8 nJ/pulse. The diameter of the laser beam was ~100 μm at the sample position, so that the photon density was estimated to be 2.5 × 10^{13} photons/cm^2 and the beam excited less than 0.1% of *p*pR molecules in the sample. Fluorescence from the *p*pR sample was collected in the same direction as the excitation beam, and the yellow glass filter (VY 48, Toshiba) cut the remaining excitation beam. The measurement with buffer solution (without the *p*pR sample) showed no signal, indicating that the observed signal originated from the fluorescence from *p*pR and no contamination of the Raman signal of water.

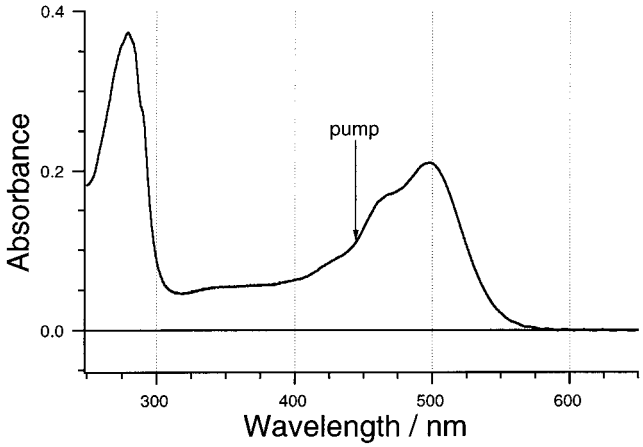

Figure 1. Absorption spectrum of *pharaonis* phoborhodopsin (*p*pR) used in the femtosecond fluorescence measurements. The λ_{max} is located at 498 nm, whose absorbance is 0.21 at a 1 mm path length. The sample is excited with a 444 nm femtosecond pulse, which is a second harmonic of the Ti:Sapphire laser output (central wavelength: 888 nm).

The residual fundamental beam (central wavelength: 888 nm) was used as a gate pulse to produce sum-frequency mixing after passing through an optical delay line controlled by a motor-driven translation stage. Two beams were focused onto a phase-matched 0.2 mm BBO crystal, which led to a formation of ultraviolet sum-frequency light. The lights other than the sum-frequency were eliminated by a combination of a filter (UG11, Melles Griot or short-filter, Asahi Bunko) and a monochromator (MC-10N, Ritsu). Finally, the UV light was detected with a photomultiplier (R585S, Hamamatsu Photonics) coupled to a single-photon counting apparatus (C-1231, Hamamatsu Photonics). The present instrumental response function was obtained by measuring the cross-correlation between the excitation and gate pulses to be a Gaussian-shape whose half width was 180 fs.

Results and Discussion

A. Fluorescence Decay Kinetics of *p*pR. Figure 1 shows the absorption spectrum of the *p*pR sample for the femtosecond time-resolved fluorescence measurement. The spectrum possesses an absorption maximum at 498 nm with a shoulder at ~460 nm, which is characteristic for *p*pR.[19] We excited the *p*pR sample at 444 nm and probed fluorescence emission at about 10 wavelengths between 488 and 687 nm. Lutz recently reported a fluorescence emission spectrum of *p*pR, which has an emission maximum at around 630 nm and where the fluorescence extends to about 850 nm.[19] Thus, the present time-resolved fluorescence measurement lacks information of the longer wavelength tail of the emission spectrum because of the limited experimental conditions.

We applied femtosecond time-resolved fluorescence spectroscopy to the present *p*pR sample. It is noted that the present excitation provides considerable excess energy to the retinal chromophore, which could affect the excited-state dynamics of the *p*pR sample. Nevertheless, we did not observe the rise-signal

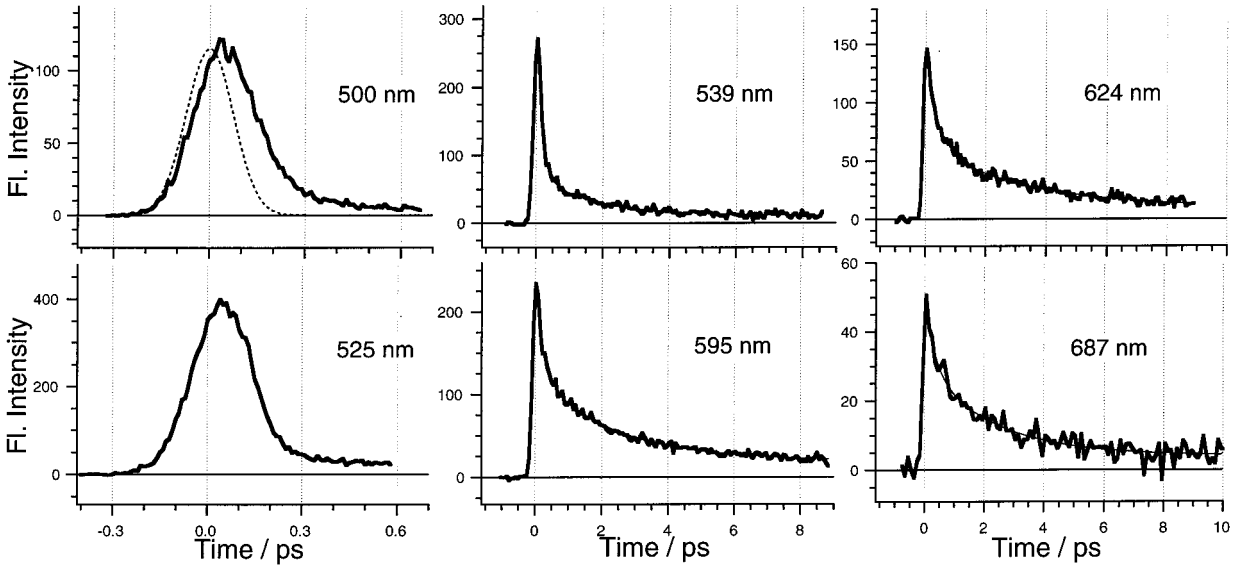

Figure 2. Fluorescence decay of *pharaonis* phoborhodopsin (*p*pR) observed at the respective wavelengths (500−687 nm). Each point is normally a sum of three kinetic traces, in which integration time is 1 s per point, whereas only the kinetics at 687 nm is obtained to be a sum of 15 kinetic traces. The instrumental response function obtained by cross-correlation measurement is superimposed (broken line at 500 nm). Thin smooth curves at 539, 595, 624, and 687 nm represent the best fit of the decays. The lifetimes and amplitudes of the fluorescence decay components are listed in Table 1.

TABLE 1: Fluorescence Lifetimes of *p*pR at the Respective Wavelengths

probing wavelength	A1 (%)	τ1 (ps)	A2 (%)	τ2 (ps)	A3 (%)	τ3 (ps)
488 nm	95	0.12 ± 0.05	5	>2		
500 nm	95	0.08 ± 0.05	5	>2		
513 nm	95	0.06 ± 0.05	5	>2		
525 nm	95	0.08 ± 0.05	5	>2		
539 nm	81	0.10 ± 0.05	16	1.7 ± 0.2	3	>10
567 nm	70	0.15 ± 0.05	26	2.1 ± 0.2	4	>10
595 nm	50	0.22 ± 0.10	42	2.3 ± 0.2	8	>10
624 nm	55	0.25 ± 0.10	38	3.0 ± 0.3	7	>10
687 nm	43	0.25 ± 0.15	49	2.3 ± 0.5	8	>10

of fluorescence at the observed wavelengths, which is normally expected in the process accompanying dynamic Stokes shift. Therefore, the observed dynamics are not significantly influenced by the excess energy.

The fluorescence kinetics from *p*pR strongly depend on the observing wavelength; the longer the probing wavelength, the longer the lifetime, as is summarized in Table 1. Figure 2 shows the typical kinetic features of *p*pR. Both at 500 and 525 nm, which correspond to 320 and 330 nm as the sum-frequency light, respectively, the fluorescence signals decay very rapidly, which are comparable with the instrumental response (broken line at 500 nm). The deconvoluted fluorescence lifetime was estimated to be 80 fs for both 500 and 525 nm kinetics. A small fluorescence signals (<5%) remained after the rapid decay, whose lifetimes are >2 ps.

The slower kinetic components are prominently observed at a longer wavelength. It is noted that the decay kinetics are clearly nonexponential at >530 nm and possibly fitted by three exponentials: (i) 100−250 fs, (ii) 1.7−3.0 ps, and (iii) > 10 ps. The third component could originate from an impurity contained in the present sample, because it gradually increased when the sample was excited repeatedly. This must be contained in the >2 ps component at 488−525 nm (Table 1). Between two major decay components, the picosecond component increased at a longer wavelength. At 687 nm, the longer wavelength side of the emission maximum (650 nm), the 2.3 ps component is greater in amplitude than the 250 fs component.

Lutz et al. recently studied primary photoreaction processes of *p*pR by means of pump−probe spectroscopy with ∼30 fs resolution.[19] They observed the ground-state depletion recovering with time constants of ∼300 fs and ∼5 ps. On the basis of a global fitting of kinetic data at wavelengths between 400 and 890 nm, they obtained three time constants within the picosecond time domain: <150 fs, 300−400 fs, and 4−5 ps. They attributed the two components in femtoseconds to the excited-state species, because the stimulated emission decayed with a time constant of 300 fs. The femtosecond components (60−250 fs) in the present fluorescence spectroscopy are coincident with those by pump−probe spectroscopy (<150 fs and 300−400 fs). Lutz et al. also assigned the 4−5 ps component as the transition from the J intermediate to the K intermediate, because the transient spectra and the time constant are similar to those for BR.[19] The present study clearly showed the presence of an additional picosecond component (1.7−3.0 ps) as the excited-state lifetime. Lack of this component in the pump−probe spectroscopy is unclear. It might be involved in the process of the 4−5 ps component, although the spectra show typical differences between intermediates and *p*pR. A slower recovering time of the ground-state depletion (∼5 ps)[19] could correspond to the picosecond component in the present fluorescence spectroscopy. Presence of the early picosecond components in the fluorescence spectroscopy and their lack in the pump−probe spectroscopy were also seen for visual rhodopsin.[5,23,24] Thus, overlapping of various spectral features in the pump−probe spectroscopy may prevent us from observing slow excited-state processes.

Because the ground-state product (J intermediate) appears with a time constant of 300 fs in the pump−probe spectroscopy of *p*pR,[19] the femtosecond component (60−250 fs) in the present study corresponds to the product formation of the J intermediate. On the other hand, no clear signal of product formation was observed in the picosecond time domain in the pump−probe spectroscopy,[19] suggesting that the picosecond component is not coupled with product formation. It is noted that such an unreactive excited state was observed in the pump−probe spectroscopy of hR.[25] An unreactive excited state was also

proposed by fluorescence spectroscopy of visual rhodopsin.[24] In these cases, the mechanisms were explained by a branching model, where the photoexcited molecule proceeds from the Franck−Condon state into the reaction coordinate (=photoisomerization) or the unreactive relaxation pathway.[5,24,25]

Du et al. previously measured time-resolved fluorescence spectroscopy of bR, and obtained three kinetic components as the excited-state lifetimes: (i) 90−240 fs, (ii) 0.6−0.9 ps, and (iii) 9−13 ps.[26] The fastest components are very close to those of *p*pR in the present study, whereas there are considerable differences in the second and third components. The second component is faster in bR (0.6−0.9 ps) than in *p*pR (1.7−3.0 ps). In addition, the amplitude of the third component is much greater in bR than in *p*pR. In fact, the amplitude of the 9−10 ps components at 770−800 nm are 25−27% for bR,[26] whereas such a longer component is lower than 10% for *p*pR (Table 1). The present study showed that the >10 ps component increased when the *p*pR sample was excited repeatedly. In addition, the *p*pR sample was solubilized by detergent, whereas the membrane fraction was used as the bR sample.[26] These facts suggest that a considerable amount of the 9−13 ps component in bR may not originate from the excited state of bR.

The origin of the nonexponential kinetics in the primary process of bR has been of great interest, though the mechanism is not clear.[27−31] It is noted that product formation of the J intermediate was only observed accompanying the ∼200 fs process and not at ≥500 fs in the pump−probe spectroscopy of bR.[27,31] This implies that the fastest component (∼200 fs) is coupled to efficient photoisomerization, whereas slower components are correlated with deactivation processes back to the ground state. This view is likely to be common among rhodopsins, such as bR, hR, *p*pR, and visual rhodopsin.

B. Kinetic Comparison of *p*pR with AT-PSB in Methanol. AT-PSB in solution is a good reference system for the present study of *p*pR. In proteins, the PSB molecule interacts specifically with surrounding amino acid residues fixed into the protein coordinate. On the other hand, in solution, surrounding solvent molecules possess a greater degree of freedom than amino acid residues of proteins. Thus, it is of interest to compare excited-state dynamics of the chromophore in *p*pR and in solution. *p*pR possesses absorption and emission maxima at 500 and 630 nm, respectively.[19] On the other hand, AT-PSB in methanol possesses absorption and emission maxima at 445 and 655 nm, respectively.[13] Emission spectra are similar between *p*pR and AT-PSB in methanol.

Figure 3 shows a kinetic comparison of the fluorescence decays of *p*pR and AT-PSB in methanol at 605 (a) and ∼690 nm (b). At 605 nm, the shorter wavelength side of the emission maximum, the decay kinetics of *p*pR and AT-PSB in methanol look apparently similar, exhibiting nonexponential decays. On the other hand, kinetics at the longer wavelength side of the emission maximum are remarkably different as shown in Figure 3b. The decay process of AT-PSB in methanol can be fitted by a single exponential, whereas that of *p*pR is highly nonexponential. We previously showed that the decay kinetics are fitted by a single exponential at the longer wavelength side of the emission maximum of AT-PSB in methanol.[13] On the other hand, the presence of the femtosecond component (60−250 fs) is characteristic in *p*pR throughout 480−700 nm. Unfortunately, we could not measure time-resolved fluorescence at the longer wavelength tail of the emission spectrum (700−900 nm) in the present study. However, the recent pump−probe spectroscopy of *p*pR clearly showed the presence of the 300 fs component as the stimulated emission decay at 890 nm.[19] Thus, the presence

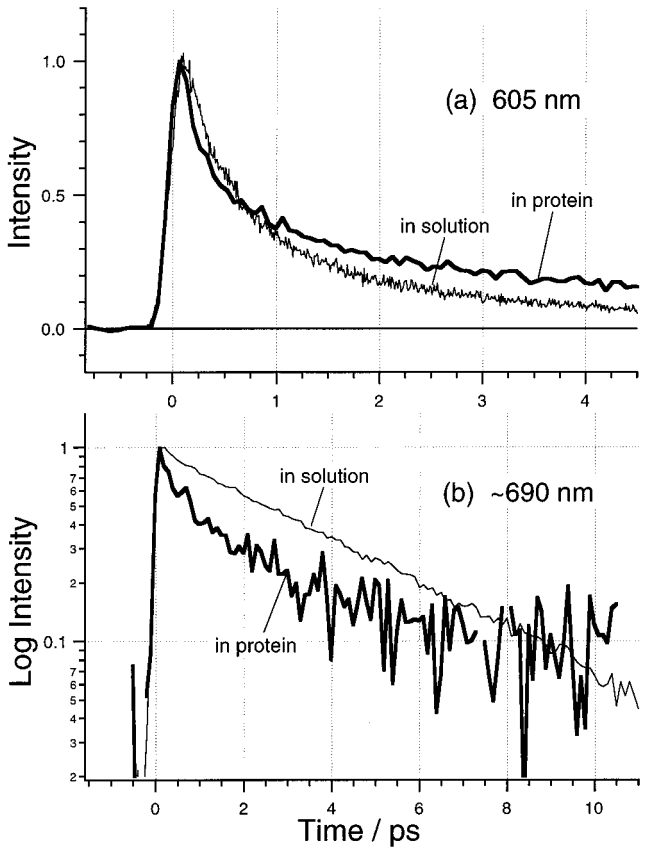

Figure 3. Kinetic comparison of the fluorescence decay between *pharaonis* phoborhodopsin (*p*pR) and a protonated Schiff base of all-trans retinal in methanol (AT-PSB).

of the femtosecond components throughout the emissive wavelength region is characteristic in the protein environment. Similar observation was reported for bR,[26] visual rhodopsin,[24] and photoactive yellow protein.[32,33]

It is generally accepted that photoisomerization is efficient in proteins. In fact, the quantum yield of *p*pR (0.5)[9] is greater than that of AT-PSB in methanol (∼0.15[10−12]). Thus, the different quantum yield between *p*pR and AT-PSB in methanol presumably originates from the population of the primary femtosecond components. In other words, as described above, femtosecond and picosecond decay processes are different in their mechanisms. The femtosecond components correspond to highly efficient photoisomerization in the excited state whose quantum yield is close to unity. In view of the time scale, the excited-state dynamics is likely to proceed through barrierless transition. On the other hand, picosecond components are correlated with deactivation processes back to the ground state of *p*pR, whose isomerization quantum yield is low. A highly organized protein matrix could concentrate the excited molecules into the reaction coordinate for photoisomerization.

Regarding specific reaction processes in protein, one notable aspect is that photoisomerization of the retinal chromophore can take place even at very low temperatures such as 4 K. This fact implies that the protein environment facilitates retinal isomerization without large motion of protein itself. Although the protein structure surrounding the retinal chromophore had not been known, progress in structural biology allowed for the determination of the structure of bR[34,35] and visual rhodopsin[36] recently. Although the structure of *p*pR is unknown at present, comparative investigation of infrared spectroscopy of *p*pR and bR has provided various structural aspects.[37] Thus, specifically

controlled photoisomerization processes in protein will be explained by structural background in the future.

Acknowledgment. This work was done in the Frontier Research Program, The Institute of Physical and Chemical Research (RIKEN), Wako, Saitama 351-01, Japan. This work was partly supported by grants for the "Special Researchers' Basic Science Program" from the Science and Technology Agency of the Japanese Government and from the Japanese Ministry of Education, Culture, Sports, Science and Technology.

Note Added in Proof. X-ray crystallographic structures of *p*pR have reported from two groups independently (Luecke et al. *Science* **2001**, *293*, 1499; Royant et al. *Proc. Natl. Acad. Sci.* **2001**, *98*, 10131). Interestingly, the structure of *p*pR was very similar to that of bR.

References and Notes

(1) Birge, B. B. *Biochim. Biophys. Acta* **1990**, *1016*, 293.
(2) Yoshizawa, T.; Kandori, H. *Progress in Retinal Research*; Pergamon Press: Oxford, 1992; Vol. 11, Chapter 2.
(3) Kochendoerfer, G. G.; Mathies, R. A. *Isr. J. Chem.* **1995**, *35*, 211.
(4) Lanyi, J. K. *J. Phys. Chem. B* **2000**, *104*, 48.
(5) Kandori, H.; Shichida, Y.; Yoshizawa, T. *Biochemistry (Moscow)* **2001**, *66*, 1197.
(6) Dartnall, H. J. A. *Vision Res.* **1967**, *8*, 339.
(7) Tittor, J.; Oesterhelt, D. *FEBS Lett.* **1990**, *263*, 269.
(8) Zhang, H.; Mauzerall, D. *Biophys. J.* **1996**, *71*, 381
(9) Losi, A.; Wegener, A. A.; Engelhard, M.; Gartner, W.; Braslavsky, S. E. *Biophys. J.* **1999**, *77*, 3277.
(10) Becker, R. S.; Freedman, K. A. *J. Am. Chem. Soc.* **1985**, *107*, 1477.
(11) Freedman, K. A.; Becker, R. S. *J. Am. Chem. Soc.* **1986**, *108*, 2169.
(12) Koyama, Y.; Kubo, K.; Komori, M.; Yasuda, H.; Mukai, Y. *Photochem. Photobiol.* **1991**, *54*, 433.
(13) Kandori, H.; Sasabe, H. *Chem. Phys. Lett.* **1993**, *216*, 126.
(14) Kandori, H.; Katsuta, Y.; Ito, M.; Sasabe, H. *J. Am. Chem. Soc.* **1995**, *117*, 2669.
(15) Sasaki, J.; Spudich, J. L. *Biochim. Biophys. Acta* **2000**, *1460*, 230.
(16) Imamoto, Y.; Shichida, Y.; Hirayama, J.; Tomioka, H.; Kamo, N.; Yoshizawa, T. *Biochemistry* **1992**, *31*, 2523.
(17) Takahashi, T.; Yan, B.; Mazur, P.; Nakanishi, K.; Spudich, J. L. *Biochemistry* **1990**, *29*, 8467.
(18) Hirayama, J.; Imamoto, Y.; Shichida, Y.; Tomioka, H.; Kamo, N.; Yoshizawa, T. *Biochemistry* **1992**, *31*, 2093.
(19) Lutz, I.; Wegener, A. A., Engelhard, M.; Boche, I.; Otsuka, M.; Oesterhelt, D.; Wachtveitl. J.; Zinth, W. *Proc. Natl. Acad. Sci. U.S.A.* **2001**, *98*, 962.
(20) Tomioka, H.; Sasabe, H. *Biochim. Biophys. Acta* **1995**, *1234*, 261.
(21) Kandori, H.; Sasabe, H.; Mimuro, M. *J. Am. Chem. Soc.* **1994**, *116*, 2671.
(22) Kandori, H.; Sasabe, H.; Nakanishi, K.; Yoshizawa, T.; Mizukami, T.; Shichida, Y. *J. Am. Chem. Soc.* **1996**, *118*, 1002.
(23) Chosrowjan, H.; Mataga, N.; Shibata, Y.; Tachibanaki, S.; Kandori, H.; Shichida, Y.; Okada, T.; Kouyama, T. *J. Am. Chem. Soc.* **1998**, *120*, 9706.
(24) Kandori, H.; Furutani, Y.; Nishimura, S.; Shichida, Y.; Chosrowjan, H.; Shibata, Y.; Mataga, N. *Chem. Phys. Lett.* **2001**, *334*, 271.
(25) Kandori, H.; Yoshihara, K.; Tomioka, H.; Sasabe, H. *J. Phys. Chem.* **1992**, *96*, 6066.
(26) Du, M.; Fleming, G. R. *Biophys. Chem.* **1993**, *48*, 101.
(27) Kandori, H.; Yoshihara, K.; Tomioka, H.; Sasabe, H.; Shichida, Y. *Chem. Phys. Lett.* **1993**, *211*, 385.
(28) Haran, G.; Wynne, K.; Xie, A.; He, Q.; Chance, M.; Hochstrasser, R. M. *Chem. Phys. Lett.* **1996**, *261*, 389.
(29) Hasson, K. C.; Gai, F.; Anfinrud, P. A. *Proc. Natl. Acad. Sci. U.S.A.* **1996**, *93*, 15124.
(30) Gai, F.; Hasson, K. C.; McDonald, J. C.; Anfinrud, P. A. *Science* **1998**, *279*, 1886.
(31) Dobler, J.; Zinth, W.; Kaiser, W.; Oesterhelt, D. *Chem. Phys. Lett.* **1988**, *144*, 215.
(32) Chosrowjan, H.; Mataga, N.; Shibata, Y.; Imamoto, Y.; Tokunaga, F. *J. Phys. Chem. B* **1998**, *102*, 7695.
(33) Mataga, N.; Chosrowjan, H.; Shibata, Y.; Imamoto, Y.; Tokunaga, F. *J. Phys. Chem. B* **2000**, *104*, 5191.
(34) Luecke, H.; Schobert, B.; Richter, H.-T.; Cartailler, J. P.; Lanyi, J. K. *J. Mol. Biol.* **1999**, *291*, 899.
(35) Belrhali, H.; Nollert, P.; Royant, A.; Menzel, C.; Rosenbusch, J. P.; Landau, E. M.; Pebay-Peyroula, E. *Structure* **1999**, *7*, 909.
(36) Palczewski, K.; Kumasaka, T.; Hori, T.; Behnke, C. A.; Motoshima, H.; Fox, B. A.; Le Trong, I.; Teller, D. C.; Okada, T.; Stenkamp, R. E.; Yamamoto, M.; Miyano, M. *Science* **2000**, *289*, 739.
(37) Kandori, H.; Shimono, K.; Sudo, Y.; Iwamoto, M.; Shichida, Y.; Kamo, N. *Biochemistry* **2001**, *40*, 9238.